CrossMark

RESEARCH ARTICLE

Near-infrared light treatment reduces astrogliosis in MPTP-treated monkeys

Nabil El Massri[1] · Cécile Moro[2] · Napoleon Torres[2] · Fannie Darlot[2] · Diane Agay[2] ·
Claude Chabrol[2] · Daniel M. Johnstone[3] · Jonathan Stone[3] · Alim-Louis Benabid[2] ·
John Mitrofanis[1]

Abstract We have reported previously that intracranial application of near-infrared light (NIr) reduces clinical signs and offers neuroprotection in a subacute MPTP (1-methyl-4-phenyl-1,2,3,6-tetrahydropyridine) monkey model of Parkinson's disease. In this study, we explored whether NIr reduces the gliosis in this animal model. Sections of midbrain (containing the substantia nigra pars compacta; SNc) and striatum were processed for glial fibrillary acidic protein (to label astrocytes; GFAP) and ionised calcium-binding adaptor molecule 1 (to label microglia; IBA1) immunohistochemistry. Cell counts were undertaken using stereology, and cell body sizes were measured using ImageJ. Our results showed that NIr treatment reduced dramatically (~75 %) MPTP-induced astrogliosis in both the SNc and striatum. Among microglia, however, NIr had a more limited impact in both nuclei; although there was a reduction in overall cell size, there were no changes in the number of microglia in the MPTP-treated monkeys after NIr treatment. In summary, we showed that NIr treatment influenced the glial response, particularly that of the astrocytes, in our monkey MPTP model of Parkinson's disease. Our findings raise the possibility of glial cells as a future therapeutic target using NIr.

Keywords Substantia nigra · Striatum · Parkinson's disease · Photobiomodulation · 670 nm

Abbreviations

ATP	Adenosine triphosphate
GFAP	Glial fibrillary acidic protein
GP	Globus pallidus
IBA1	Ionised calcium-binding adaptor molecule 1
MPTP	1-Methyl-4-phenyl-1,2,3,6-tetrahydropyridine
NIr	Near-infrared light
R	Red nucleus
SNc	Substantia nigra pars compacta
SNr	Substantia nigra pars reticulata

✉ John Mitrofanis
john.mitrofanis@sydney.edu.au

Nabil El Massri
nabil.elmassri@sydney.edu.au

Cécile Moro
cecile.moro@cea.fr

Napoleon Torres
napoleon.torres-martinez@cea.fr

Fannie Darlot
fannie.darlot@cea.fr

Diane Agay
diane.agay@cea.fr

Claude Chabrol
cl.chabrol@cea.fr

Daniel M. Johnstone
daniel.johnstone@sydney.edu.au

Jonathan Stone
jonathan.stone@sydney.edu.au

Alim-Louis Benabid
alimlouis@sfr.fr

[1] Department of Anatomy F13, University of Sydney, Sydney 2006, Australia

[2] University Grenoble Alpes, CEA, LETI, CLINATEC, MINATEC Campus, 38000 Grenoble, France

[3] Department of Physiology F13, University of Sydney, Sydney 2006, Australia

Introduction

Gliosis is the hypertrophy or proliferation of glial cells in response to neural damage by either stroke, trauma or neurodegenerative disease. Historically, gliosis has been associated with toxic, detrimental effects on neurones, by either inhibiting axonal regeneration by forming glial scars and/or secreting pro-inflammatory cytokines and other neurotoxic products. More recently, gliosis has also been associated with more beneficial effects after damage, for example with the release of neuroprotective agents such as glial-derived neurotrophic factor. The relationship between toxic and beneficial function appears complex, being dependent on an array of different factors and molecular signalling mechanisms, and may change with time period after the injury (McGeer and McGeer 1998, 2008; Barcia et al. 2003; Hamby and Sofroniew 2010; Halliday and Stevens 2011; Pekny et al. 2014; Pekny and Pekna 2014; Verkhratsky et al. 2014; Burda et al. 2016).

Parkinson's disease is a major neurodegenerative movement disorder and is characterised by, not only a progressive loss of dopaminergic neurones in the substantia nigra pars compacta (SNc) and their terminations in the striatum (Blandini et al. 2000; Bergman and Deuschl 2002), but also a massive gliosis, particularly of astrocytes and microglia, the two major forms of glia (McGeer and McGeer 1998, 2008; Barcia et al. 2003).

Recently, we have shown that after application of the neuroprotective agent near-infrared light (NIr), there is a reduction in clinical signs and an increase in dopaminergic neurone survival in a monkey model (MPTP; 1-methyl-4-phenyl-1,2,3,6-tetrahydropyridine) of Parkinson's disease (Darlot et al. 2016). In that study, NIr was delivered intracranially to a midline midbrain region close to the degenerative dopaminergic neurones in the SNc. Although the precise mechanism of NIr-induced neuroprotection is not clear, recent evidence indicates that NIr is a low-level stressor of cells and that activation of endogenous cellular stress responses is likely to be central to its efficacy (Chung et al. 2012; Rojas and Gonzalez-Lima 2011; Khan and Arany 2015). The main target of NIr appears to be cytochrome c oxidase, a key enzyme of the mitochondrial respiratory chain. This enzyme is a photoacceptor of light in the NIr range; NIr generates a redox change in cytochrome c oxidase that causes a transient change in mitochondrial membrane potential, leading to an increase in ATP (adenosine triphosphate) production and a burst in low levels of reactive oxygen species (Chung et al. 2012; Rojas and Gonzalez-Lima 2011; Begum et al. 2013; Gkotsi et al. 2014; Khan and Arany 2015). This, in turns, triggers a cascade of secondary downstream signalling pathways that collectively stimulate endogenous cell protection and repair

mechanisms (Chung et al. 2012; Rojas and Gonzalez-Lima 2011; Khan and Arany 2015).

In the present study, we took the opportunity to examine this rare primate material further, by analysing the patterns of gliosis in our monkey MPTP model and after NIr treatment. We explored the organisation of astrocytes and microglia in both the SNc and striatum, the major regions of lesion after MPTP insult. We aimed to provide insight into the impact of NIr on the morphological aspects of the glial response after MPTP insult, to hopefully understand better how NIr offers neuroprotection in primates.

Methods

The brains of twenty-two adult Macaque monkeys (Macaca fascicularis) aged 4–5 years, weighing 5–7 kg, were analysed. All the experiments were approved by the Animal Ethics Committee COMETH (Grenoble), by the French Ministry for Research (protocol number 00562.02) and were performed in accordance with the European Communities Council Directive of 1986 (86/609/EEC) for care of laboratory animals.

These animals formed part of a larger study exploring the impact of NIr on the behaviour and survival of cells in the SNc and their terminations in the striatum (Darlot et al. 2016); there was no overlap of results between the present study and the previous one. In the previous study (Darlot et al. 2016), full details of the NIr optical fibre device and the entire experimental procedure were described; hence, only the major points of protocol will be outlined here.

We analysed the SNc and striatum of monkeys in three groups: (1) Control (n = 5): animals that received no MPTP treatment. Three monkeys had an optical fibre implant (but not activated) into the midbrain (see below), while two were left intact. We have shown that neither the surgical procedure nor optical fibre implant had any impact on behaviour and/or dopaminergic neurone number (Darlot et al. 2016) (2) MPTP (n = 11): animals that received MPTP injections over five or seven days (subacute MPTP model; Ashkan et al. 2007; Wallace et al. 2007; Darlot et al. 2016; Fig. 1); ten of these monkeys were left intact, and one had an optical fibre implant (not activated). There were no differences in the clinical scores nor dopaminergic neurone loss between the monkeys given different doses of MPTP; hence, the data were pooled (Darlot et al. 2016) (3) MPTP-NIr (n = 6): animals that received MPTP injections as above, in conjunction with optical fibre implants delivering NIr (Fig. 1). These monkeys formed the MPTP-NIr1 group of our previous study (Darlot et al. 2016), the group that showed few clinical signs and had clear evidence of neuroprotection. We chose this group for inclusion because
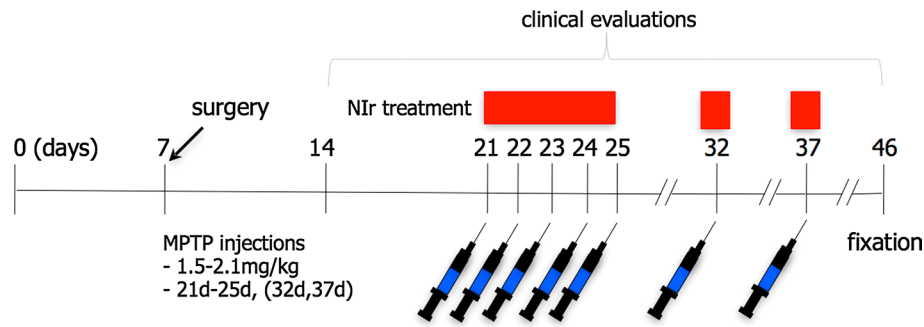
Fig. 1 Outline of the overall experimental design of monkeys used in this study. We are used material from the larger study of Darlot et al. (2016). There are three experimental groups. The Control group has no NIr treatment nor MPTP injections. The MPTP group has either 1.5 mg/kg MPTP administered over 5 days (days 21–25; major period of MPTP injections) or 2.1 mg/kg MPTP administered over 7 days (days 21–25, 32, 37; there are no differences in clinical signs nor neuronal survival between the two dose regimes; Darlot et al. 2016). The MPTP-NIr group has the same MPTP dose regimes, together with two NIr dosages (25 or 35 J; 5 s ON/60 s OFF over the 24-h period after each MPTP injection). For the MPTP-NIr group, monkeys have optical fibres implanted surgically into the midbrain and MPTP injections are administered 2 weeks thereafter (day 21). The clinical evaluation of each monkey is started a week after surgery (day 14). At the end of the experimental period, monkeys are perfused transcardially and processed for immunohistochemistry (day 46). It should be noted that one monkey of the MPTP group and three monkeys of the Control group have optical fibre implants; all other monkeys of these groups are left intact

it would provide the clearest indication of whether NIr had an impact on gliosis after MPTP insult.

Many of the animals were implanted stereotactically with a NIr optical fibre that was attached proximally to a 670 nm laser diode that was itself connected to the battery of an implantable stimulator. We targeted stereotactically a region close to the midline of the midbrain, near the SNc of both sides. After implantation, the skull opening was filled with biological cement and the overlying tissues were sutured (Moro et al. 2014; Reinhart et al. 2015; Darlot et al. 2016). Animals in the MPTP and MPTP-NIr groups received intramuscular MPTP injections (0.3 mg/kg/day; Sigma) for either five (total of 1.5 mg/kg) or seven (total of 2.1 mg/kg) days (Fig. 1). Monkeys in the MPTP-NIr group had the NIr device turned on (5 s ON/60 s OFF) a few minutes before each MPTP injection; the device remained turned on for the next 24-h period (Fig. 1). The output was 10 mW power, resulting in an estimated total dose of 25–35 J (Darlot et al. 2016). Twenty-four hours after the last MPTP injection, the device was turned off. During the bulk of the experimental period, from a week after surgery up until termination (i.e. 32 days; Fig. 1), monkeys were evaluated clinically using a modified J.S. Schneider scale, measuring a range of parameters, for example from posture to general activity and from facial expression to bradykinesia (Schneider et al. 2003; Darlot et al. 2016).

At the end of the experimental period, animals were anaesthetised with intramuscular injections of sodium pentobarbital (60 mg/kg) and had their brains aldehyde-fixed, cryoprotected and sectioned using a freezing microtome. Sections of midbrain and striatum (1/5 series) were incubated in either anti-glial fibrillary acidic protein (to label astrocytes; GFAP; 1:500; Z033429-2 Dako) or anti-ionised calcium-binding adaptor molecule 1 (to label microglia; IBA1; 1:500; 019-19741 Wako) followed by biotinylated anti-rabbit IgG and then Extravidin–peroxidase complex (1:20 EXTRA3-1KT Sigma). Sections were reacted in a 3,3′-diaminobenzidine tetrahydrochloride solution (D3939 Sigma) and then coverslipped. The midbrain sections were counterstained lightly with neutral red, as to reveal the nuclear boundaries of the SNc. For controls, sections were processed as described above except that no primary antibody was used. These control sections were immunonegative. The number of glial cells in the SNc and striatum was estimated using the optical fractionator method (StereoInvestigator, MBF Science) as described by previous studies (Shaw et al. 2010; Peoples et al. 2012; Moro et al. 2014; Johnstone et al. 2014; Reinhart et al. 2015; Darlot et al. 2016; El Massri et al. 2016). The cell body size of glia in the SNc and striatum was measured using ImageJ software. The cell bodies were traced from photomicrographs and the programme calculated the area of each cell (~20 cells from each animal). The results from the MPTP and MPTP-NIr groups are presented as a percentage difference in size relative to the Control group. One-way ANOVA was used for statistical group comparisons of immunoreactive cell numbers (GraphPad Prism).

Results

Our results on the patterns of GFAP and IBA1 immunoreactivity will be considered separately. Figure 2a shows a graph of the estimated total number of GFAP⁺ astrocytes

in the SNc (black columns) and striatum (grey columns) of monkeys in the different experimental groups. There were clear differences in the number of GFAP$^+$ astrocytes in both the SNc and striatum of the different groups. In both nuclei, there were 80–90 % more astrocytes in the MPTP group than in the Control. In the MPTP-NIr group, astrocyte number had reduced by ~75 % from the MPTP group, to near control levels (Fig. 2a). The differences in number between the groups were significant, for both the SNc (ANOVA: $F = 19$; $p < 0.0001$) and for the striatum (ANOVA: $F = 14$; $p < 0.0001$).

The photomicrographs in Fig. 2b–g extend further the patterns described above for the SNc (Fig. 2b, d, f) and striatum (Fig. 2c, e, g). In the Control group, there were many finely labelled fibres, but few GFAP$^+$ cells in both the SNc (arrow Fig. 2b) and striatum (arrow Fig. 2c). In the MPTP group, a very different pattern was evident, with both nuclei being characterised by numerous, strongly labelled GFAP$^+$ astrocytes (arrows Fig. 2d, e). In the MPTP-NIr group, GFAP immunoreactivity resembled the control monkeys, with a much sparser distribution of GFAP$^+$ astrocytes—compared to the MPTP group—being seen across both nuclei (arrows Fig. 2f, g). The graph in Fig. 2h indicates that there were also clear differences in the size of the GFAP$^+$ cell bodies between the groups; astrocytes in the MPTP group were considerably larger—and presumably activated—than those in the Control and MPTP-NIr group of both nuclei. The differences in cell body size between the groups were significant in the SNc (ANOVA: $F = 72$; $p < 0.0001$) and the striatum (ANOVA: $F = 103$; $p < 0.0001$).

For the IBA1$^+$ microglia, the graph in Fig. 3a shows that differences in the estimated total numbers in the SNc (black columns) and striatum (grey columns) between the experimental groups were not as clear as they were for the GFAP$^+$ astrocytes (Fig. 2a). In the SNc, the number of microglia were very similar in the different groups, while in the striatum, there was a 45–55 % increase in number in the MPTP and MPTP-NIr groups compared to Control group (Fig. 3a). The differences in number between the groups were significant for striatum (ANOVA: $F = 12$; $p < 0.0001$), but not for the SNc (ANOVA: $F = 0.3$; $p > 0.05$).

The photomicrographs in Fig. 3b–g indicate few differences in the morphology of IBA1$^+$ microglia in the SNc (Fig. 3b, d, f) and striatum (Fig. 3c, e, g). The majority of cells had small cell bodies and finely labelled processes, the classical resting appearance (McGeer and McGeer 2008; Halliday and Stevens 2011). The only substantial difference we noted in the patterns of IBA1 immunoreactivity of the different groups was in the SNc of the MPTP group, where large amoeboid-like (and presumably activated) cells were often found (arrow Fig. 3d). We never saw these cells

in the SNc of the other groups, nor in the striatum of any group. The presence of these cells in the SNc of the MPTP group presumably contributed to the substantial increase in the cell body size of the microglia compared to the Control and MPTP-NIr groups (Fig. 3h). The cell bodies of microglia in the MPTP group of the striatum were also larger than the other groups, but to a smaller extent. The differences in cell body size between the groups were significant in the SNc (ANOVA: $F = 10$; $p < 0.0001$) and the striatum (ANOVA: $F = 5.1$; $p < 0.01$).

Discussion

Previous studies have reported an increase in both astrocyte and microglia reactivity in the SNc and striatum of rodents after MPTP or 6-hydroxydopamine lesion (Francis et al. 1995; Strömberg et al. 1986; Reinhard et al. 1988; Członkowska et al. 1996; Kohutnicka et al. 1998; Fernagut et al. 2004; Johnstone et al. 2014; El Massri et al. 2016). In general, these studies indicate a proliferation of both astrocytes and microglia almost immediately after insult; thereafter, microglia tend to return to control-like levels before the astrocytes, within a matter of weeks (Członkowska et al. 1996; Kohutnicka et al. 1998). In primates, our knowledge of the glial response after parkinsonian insult is, given the rarity of the material, understandably scarce, but there are some reports on offer. In MPTP-treated monkeys (Hurley et al. 2003; McGeer et al. 2003) and Parkinson's disease patients (McGeer et al. 1988; Mirza et al. 1999), an increase in microglia reactivity has been shown in the SNc, but not the striatum (Mirza et al. 1999; Hurley et al. 2003); in Parkinson's disease patients, little if any astrocytic proliferation has been reported in the SNc and striatum (Mirza et al. 1999). It is likely that the limited astrogliosis and microgliosis reported in patients and MPTP-treated monkeys relates to the time period of examination; astrocytes and microglia may have been more active at earlier stages of the disease process in these cases, but this is yet to be determined.

Our results in MPTP-treated monkeys largely confirm and extend previous studies. We extend previous findings by showing a proliferation of reactive astrocytes in the SNc and striatum of MPTP-treated monkeys; the number and size of these cells increased from the controls. For microglia, the MPTP-treated monkeys showed an increase in number and cell size in the striatum, while in the SNc, although there was no change in number, cells were larger compared to the controls, with many having a reactive amoeboid-like morphology (see "Results"). Thus, in the time frame of our subacute MPTP model (Fig. 1), many aspects of the glia reaction after parkinsonian insult described above were captured.

Fig. 2 a Graph of the estimated number of GFAP$^+$ astrocytes in the SNc (*black columns*) and striatum (*grey columns*) in the different experimental groups. *Left-hand side Y axis* (and adjacent ANOVA test result) relates to SNc cell number, while *right-hand side Y axis* (and adjacent ANOVA test result) relates to striatal number. The *columns* show the mean ± standard error. Photomicrographs of GFAP$^+$ astrocytes (*arrows*) in the SNc (**b, d, f**) and striatum (**c, e, g**) of the control (**b, c**), MPTP (**d, e**) and MPTP-NIr (**f, g**) groups. The sections of the SNc are counterstained lightly with neutral *red*, as to reveal the boundaries of the nucleus clearly (**b, d, f**). For the SNc, each photomicrograph is taken from a central region (*inset* **b**), in sections corresponding to plate 74–75 of a monkey atlas (Paxinos et al. 1998). For the striatum, each photomicrograph is taken from a dorsal region (*inset* **c**), corresponding to plates 62 in the atlas (Paxinos et al. 1998). All figures are of coronal sections, *dorsal* to *top*, *medial* to *left*. *Scale* = 100 μm. **h** Graph of the astrocyte cell body size in the SNc (*black columns*) and striatum (*grey columns*) in the MPTP and MPTP-NIr groups. The results from these groups are presented as a percentage difference in size to the Control group
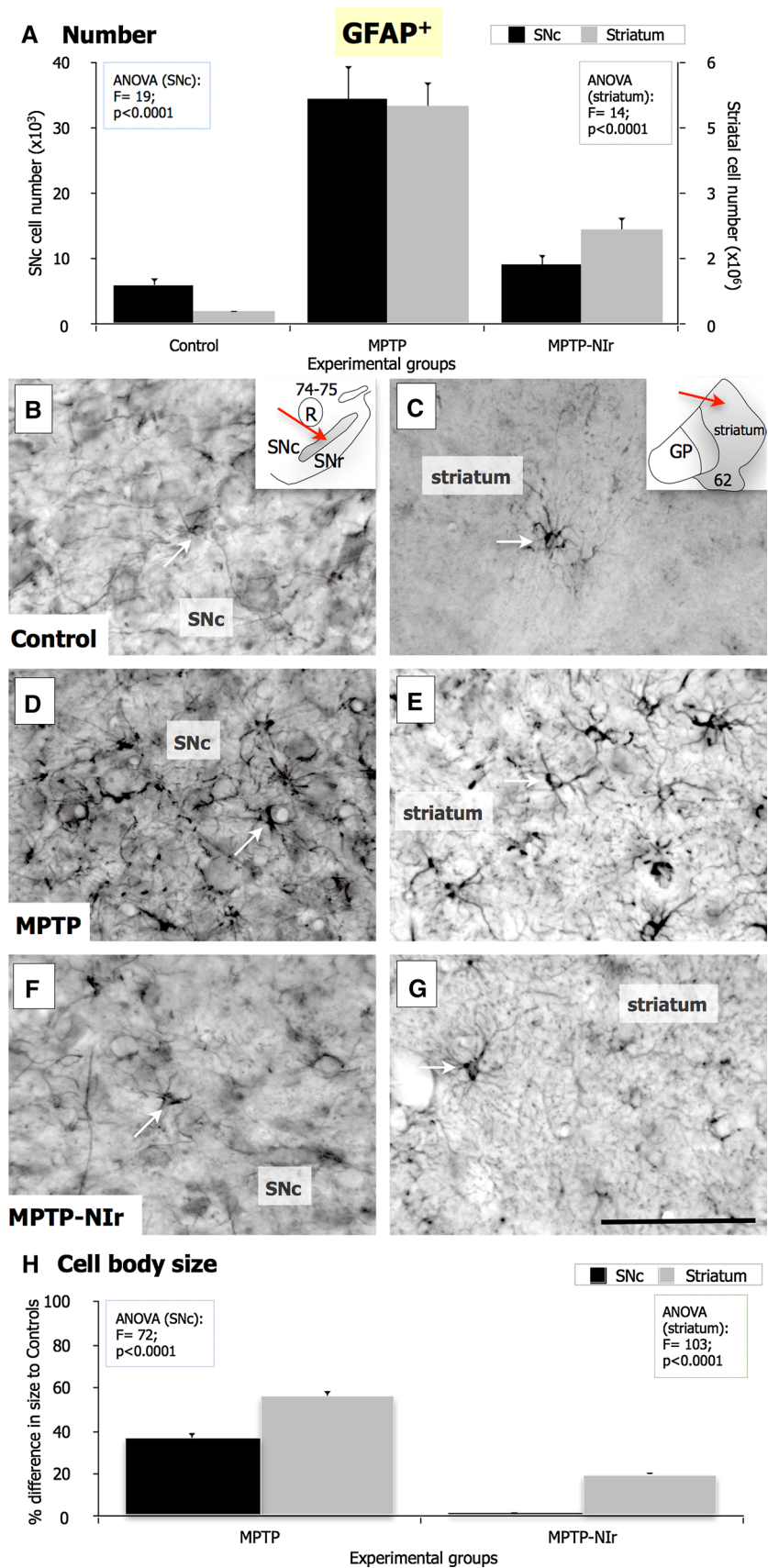
Fig. 3 a Graph of the estimated number of IBA1^{+} microglia in the SNc (*black columns*) and striatum (*grey columns*) in the different experimental groups. *Left-hand side Y axis* (and adjacent ANOVA test result) relates to SNc cell number, while *right-hand side Y axis* (and adjacent ANOVA test result) relates to striatal number. The *columns* show the mean ± standard error. Photomicrographs of IBA1^{+} microglia in the SNc (**b, d, f**) and striatum (**c, e, g**) of the Control (**b, c**), MPTP (**d, e**) and MPTP-NIr (**f, g**) groups. The sections of the SNc are counterstained lightly with *neutral red*, as to reveal the boundaries of the nucleus clearly (**b, d, f**). *Arrow* in (**d**) indicates large amoeboid-like IBA1^{+} cell; these are found only in the SNc of the MPTP group. For the SNc, each photomicrograph is taken from a central region (*inset* **b**), in sections corresponding to plate 74–75 of a monkey atlas (Paxinos et al. 1998). For the striatum, each photomicrograph is taken from a dorsal region (*inset* **c**), corresponding to plates 62 in the atlas (Paxinos et al. 1998). All figures are of coronal sections, *dorsal* to *top*, *medial* to *left*. *Scale* = 100 µm. **h** Graph of the microglia cell body size in the SNc (*black columns*) and striatum (*grey columns*) in the MPTP and MPTP-NIr groups. The results from these groups are presented as a percentage difference in size to the Control group
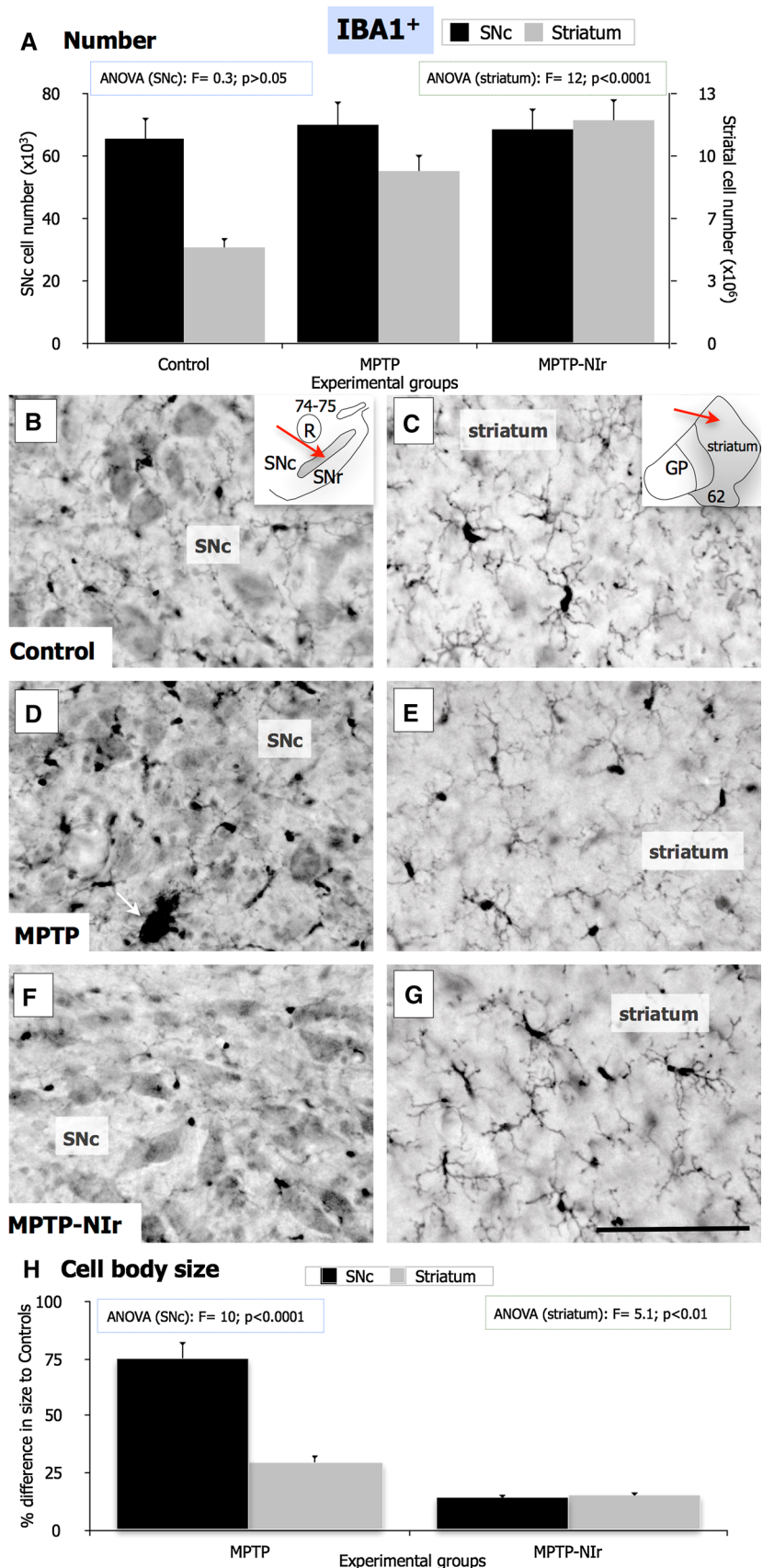
The most novel finding of this study relates to the impact of NIr on this glial response in the primate SNc and striatum. In particular, we showed that NIr treatment reduced dramatically MPTP-induced astrogliosis in both nuclei. A similar reduction in astrogliosis by NIr has been shown also in the aged mouse retina (Begum et al. 2013). Among microglia, however, our findings indicated a more limited impact by NIr in MPTP-treated monkeys; although there was a reduction in cell size (due to fewer amoeboid-like cells, at least in the SNc), there were no changes in the number of microglia after NIr treatment. We have reported a similar pattern in an acute rodent MPTP model, where NIr reduced the number of astrocytes in the striatum, but had no effect on the microglia (Johnstone et al. 2014; El Massri et al. 2016). The impact on astrocytes in the SNc in rodents was less clear, however, but this may be due to the more acute nature of the MPTP model we used (Johnstone et al. 2014). Nevertheless, NIr was clearly more effective in reducing astrogliosis than microgliosis in both primate and rodent MPTP models.

The reason for this differential effect by NIr on the two types of glia is not clear, but two possibilities suggest themselves. First, the astrocytes may have receptors or other qualities that make them generically more likely to be influenced by NIr than microglia; this feature may be unique to parkinsonian insult, however, for it appears not the case in other disorders, for example multiple sclerosis (Muili et al. 2012), aged-related macular degeneration (Rutar et al. 2015) and traumatic brain injury (Khuman et al. 2012), where microgliosis has been reported to be reduced by NIr treatment. Second, at our stage of treatment in relation to insult, astrocytes may have been more sensitive to NIr treatment than microglia; at other stages in the disease process, microglia may have been more sensitive to NIr.

In conclusion, we have shown that in a primate model of Parkinson's disease, NIr treatment reduced markedly astrogliosis in the SNc and striatum, two regions where our previous study has reported evidence for neuroprotection, an increase in dopaminergic neurone survival (Darlot et al. 2016). It is not known if this reduction in astrogliosis was due to the NIr acting on the astrocytes directly or secondary to the neuroprotection. If acting directly on the astrocytes, the NIr treatment could have stimulated a neuroprotective role for these glial cells, perhaps by triggering the cellular mechanisms outlined above (see "Introduction"), resulting in an increase in their secretion of anti-inflammatory agents and a reduction in their pro-inflammatory ones (McGeer and McGeer 2008). This, in turn, would have resulted in a greater survival of dopaminergic neurones in the SNc and their terminations in the striatum. With regard to the microgliosis, our results indicated that the impact of NIr was less distinct, but that could be due to the time frame limitations of our primate model. Future studies, particularly using cell culture models, may explore whether NIr-mediated neuroprotection involves the glial cells directly, in particular astrocytes. Overall, our results showed that NIr treatment influenced the glial response to parkinsonian insult; notwithstanding whether this influence was direct or secondary to the neuroprotection, our findings raise the possibility of glial cells as a future therapeutic target using NIr.

References

Ashkan K, Wallace BA, Mitrofanis J et al (2007) SPECT imaging, immunohistochemical and behavioural correlations in the primate models of Parkinson's disease. Parkinsonism Relat Disord 13:266–275. doi:10.1016/j.parkreldis.2006.10.009

Barcia C, Barreiro AF, Poza M, Herrero M-T (2003) Parkinson's disease and inflammatory changes. Neurotox Res 5:411–417. doi:10.1007/BF03033170

Begum R, Powner MB, Hudson N et al (2013) Treatment with 670 nm light up regulates cytochrome C oxidase expression and reduces inflammation in an age-related macular degeneration model. PLoS ONE 8:e57828. doi:10.1371/journal.pone.0057828

Bergman H, Deuschl G (2002) Pathophysiology of Parkinson's disease: from clinical neurology to basic neuroscience and back. Mov Disord 17(Suppl 3):S28–S40

Blandini F, Nappi G, Tassorelli C, Martignoni E (2000) Functional changes of the basal ganglia circuitry in Parkinson's disease. Prog Neurobiol 62:63–88

Burda JE, Bernstein AM, Sofroniew MV (2016) Astrocyte roles in traumatic brain injury. Exp Neurol 275(Pt 3):305–315. doi:10.1016/j.expneurol.2015.03.020

Chung H, Dai T, Sharma SK et al (2012) The nuts and bolts of low-level laser (light) therapy. Ann Biomed Eng 40:516–533. doi:10.1007/s10439-011-0454-7

Członkowska A, Kohutnicka M, Kurkowska-Jastrzebska I, Członkowski A (1996) Microglial reaction in MPTP (1-methyl-4-phenyl-1,2,3,6-tetrahydropyridine) induced Parkinson's disease mice model. Neurodegeneration 5:137–143

Darlot F, Moro C, El Massri N et al (2016) Near-infrared light is neuroprotective in a monkey model of Parkinson disease. Ann Neurol 79:59–75. doi:10.1002/ana.24542

El Massri N, Johnstone DM, Peoples CL et al (2016) The effect of different doses of near infrared light on dopaminergic cell survival and gliosis in MPTP-treated mice. Int J Neurosci 126:76–87. doi:10.3109/00207454.2014.994063

Fernagut PO, Diguet E, Bioulac B, Tison F (2004) MPTP potentiates 3-nitropropionic acid-induced striatal damage in mice: reference to striatonigral degeneration. Exp Neurol 185:47–62

Francis JW, Von Visger J, Markelonis GJ, Oh TH (1995) Neuroglial responses to the dopaminergic neurotoxicant 1-methyl-4-phenyl-1,2,3,6-tetrahydropyridine in mouse striatum. Neurotoxicol Teratol 17:7–12. doi:10.1016/0892-0362(94)00048-I

Gkotsi D, Begum R, Salt T et al (2014) Recharging mitochondrial batteries in old eyes. Near infra-red increases ATP. Exp Eye Res 122:50–53. doi:10.1016/j.exer.2014.02.023

Halliday GM, Stevens CH (2011) Glia: initiators and progressors of pathology in Parkinson's disease. Mov Disord 26:6–17. doi:10.1002/mds.23455

Hamby ME, Sofroniew MV (2010) Reactive astrocytes as therapeutic targets for CNS disorders. Neurotherapeutics 7:494–506. doi:10.1016/j.nurt.2010.07.003

Hurley SD, O'Banion MK, Song DD et al (2003) Microglial response is poorly correlated with neurodegeneration following chronic, low-dose MPTP administration in monkeys. Exp Neurol 184:659–668. doi:10.1016/S0014-4886(03)00273-5

Johnstone DM, El Massri N, Moro C et al (2014) Indirect application of near infrared light induces neuroprotection in a mouse model of parkinsonism—an abscopal neuroprotective effect. Neuroscience 274:93–101. doi:10.1016/j.neuroscience.2014.05.023

Khan I, Arany P (2015) Biophysical approaches for oral wound healing: emphasis on photobiomodulation. Adv Wound Care (New Rochelle) 4:724–737. doi:10.1089/wound.2014.0623

Khuman J, Zhang J, Park J et al (2012) Low-level laser light therapy improves cognitive deficits and inhibits microglial activation after controlled cortical impact in mice. J Neurotrauma 29:408–417. doi:10.1089/neu.2010.1745

Kohutnicka M, Lewandowska E, Kurkowska-Jastrzębska I et al (1998) Microglial and astrocytic involvement in a murine model of Parkinson's disease induced by 1-methyl-4-phenyl-1,2,3,6-tetrahydropyridine (MPTP). Immunopharmacology 39:167–180. doi:10.1016/S0162-3109(98)00022-8

McGeer PL, McGeer EG (1998) Glial cell reactions in neurodegenerative diseases: pathophysiology and therapeutic interventions. Alzheimer Dis Assoc Disord 12(Suppl 2):S1–S6

McGeer PL, McGeer EG (2008) Glial reactions in Parkinson's disease. Mov Disord 23:474–483. doi:10.1002/mds.21751

McGeer PL, Itagaki S, Boyes BE, McGeer EG (1988) Reactive microglia are positive for HLA-DR in the substantia nigra of Parkinson's and Alzheimer's disease brains. Neurology 38:1285–1291

McGeer PL, Schwab C, Parent A, Doudet D (2003) Presence of reactive microglia in monkey substantia nigra years after 1-methyl-4-phenyl-1,2,3,6-tetrahydropyridine administration. Ann Neurol 54:599–604. doi:10.1002/ana.10728

Mirza B, Hadberg H, Thomsen P, Moos T (1999) The absence of reactive astrocytosis is indicative of a unique inflammatory process in Parkinson's disease. Neuroscience 95:425–432. doi:10.1016/S0306-4522(99)00455-8

Moro C, El Massri N, Torres N et al (2014) Photobiomodulation inside the brain: a novel method of applying near-infrared light intracranially and its impact on dopaminergic cell survival in MPTP-treated mice. J Neurosurg 120:670–683. doi:10.3171/2013.9.JNS13423

Muili KA, Gopalakrishnan S, Meyer SL et al (2012) Amelioration of experimental autoimmune encephalomyelitis in C57BL/6 mice by photobiomodulation induced by 670 nm light. PLoS ONE 7:e30655. doi:10.1371/journal.pone.0030655

Paxinos G, Huang X, Toga A (1998) The Rhesus monkey brain in stereotaxic coordinates. Academic Press, USA

Pekny M, Pekna M (2014) Astrocyte reactivity and reactive astrogliosis: costs and benefits. Physiol Rev 94:1077–1098. doi:10.1152/physrev.00041.2013

Pekny M, Wilhelmsson U, Pekna M (2014) The dual role of astrocyte activation and reactive gliosis. Neurosci Lett 565:30–38. doi:10.1016/j.neulet.2013.12.071

Peoples C, Spana S, Ashkan K et al (2012) Photobiomodulation enhances nigral dopaminergic cell survival in a chronic MPTP mouse model of Parkinson's disease. Parkinsonism Relat Disord 18:469–476. doi:10.1016/j.parkreldis.2012.01.005

Reinhard JF Jr, Miller DB, O'Callaghan JP (1988) The neurotoxicant MPTP (1-methyl-4-phenyl-1,2,3,6-tetrahydropyridine) increases glial fibrillary acidic protein and decreases dopamine levels of the mouse striatum: evidence for glial response to injury. Neurosci Lett 95:246–251

Reinhart F, El Massri N, Darlot F et al (2015) Evidence for improved behaviour and neuroprotection after intracranial application of near infrared light in a hemi-parkinsonian rat model. J Neurosurg 27:1–13

Rojas J, Gonzalez-Lima F (2011) Low-level light therapy of the eye and brain. Eye Brain 3:49–67

Rutar M, Natoli R, Chia RX et al (2015) Chemokine-mediated inflammation in the degenerating retina is coordinated by Müller cells, activated microglia, and retinal pigment epithelium. J Neuroinflammation 12:8. doi:10.1186/s12974-014-0224-1

Schneider JS, Gonczi H, Decamp E (2003) Development of levodopa-induced dyskinesias in parkinsonian monkeys may depend upon rate of symptom onset and/or duration of symptoms. Brain Res 990:38–44

Shaw VE, Spana S, Ashkan K et al (2010) Neuroprotection of midbrain dopaminergic cells in MPTP-treated mice after near-infrared light treatment. J Comp Neurol 518:25–40. doi:10.1002/cne.22207

Strömberg I, Björklund H, Dahl D et al (1986) Astrocyte responses to dopaminergic denervations by 6-hydroxydopamine and 1-methyl-4-phenyl-1,2,3,6-tetrahydropyridine as evidenced by glial fibrillary acidic protein immunohistochemistry. Brain Res Bull 17:225–236. doi:10.1016/0361-9230(86)90119-X

Verkhratsky A, Parpura V, Pekna M et al (2014) Glia in the pathogenesis of neurodegenerative diseases. Biochem Soc Trans 42:1291–1301. doi:10.1042/BST20140107

Wallace BA, Ashkan K, Heise CE et al (2007) Survival of midbrain dopaminergic cells after lesion or deep brain stimulation of the subthalamic nucleus in MPTP-treated monkeys. Brain 130:2129–2145. doi:10.1093/brain/awm137